

APPLICATION OF MATERIAL FORCES IN DEFECT MECHANICS

R. Mueller and D. Gross

Institute of Mechanics, TU Darmstadt, D-64289 Darmstadt, Germany

ABSTRACT

Ferroelectric materials are nowadays widely used in sensor and actuator applications. Their applicability in cyclic loading however is limited by the so called 'electric fatigue' effect. Under this terminology various micro-mechanical phenomena are summarized. On the macroscopic level a reduction of the mechanical output for a fixed electric excitation is observed. One of suspected micro-mechanical mechanisms is the hindering and blocking of domain wall movement within the material. Possible sources of these blocking phenomena are point defects in the material. The point defects interact with the domain wall (inhomogeneity) and the external applied loads. Experimentally observations suggest that these point defects are oxygen vacancies. Their presence and characterization is however an experimentally difficult task. The numerical simulation is intended to provide a qualitative understanding of the interaction of point defects and domain walls. In order to model these inhomogeneities the material forces or driving forces acting on the domain wall are identified. Once the coupled field equations are solved by Finite Elements the material forces are calculated to investigate possible motions of the domain wall. At the present state the work does not incorporate a kinetic law, but is based on quasi-equilibrium considerations. The numerical simulations will demonstrate the effect of point defect position and concentration on the driving force acting on the domain wall. Eventually leading to a possible blocking of the domain wall. In order to overcome these obstacles higher external fields are necessary to move the domain wall again.

1 INTRODUCTION

To identify the material forces acting on domain walls a variational procedure will be presented which takes variations with respect to the fields and the domain wall position into account. As a result of the variational procedure the field equations and the material forces, also termed driving force in the following, are derived. For a general introduction to the theory of material forces see [1–3]. The variational procedure can also be used to derive the discretized field equations within a Finite Element setting. Details are omitted here for the sake of brevity. For a discussion of material forces in the context of Finite Element discretizations see for example [4, 5].

Examples will demonstrate the interaction of point defects with a single domain wall. It will be shown that point defects are capable of blocking a domain wall, i.e. that

the driving force acting on the domain wall is reduced. This effect is experimentally observed, see for example [6].

2 VARIATIONAL PROCEDURE

We assume that the body under consideration \mathcal{B} contains a domain wall \mathcal{S} which separates the body into two domains \mathcal{B}^+ and \mathcal{B}^- . The normal $\mathbf{n}_\mathcal{S}$ to the domain wall \mathcal{S} points from the domain \mathcal{B}^- into \mathcal{B}^+ , see fig. 1 for details. The domain wall is assumed to be a perfect interface, where the jump in the displacements $\llbracket \mathbf{u} \rrbracket = \mathbf{0}$ and the jump in the electric potential $\llbracket \varphi \rrbracket = 0$. In a purely mechanical context a similar derivation can be found in [7]. The electric enthalpy H is introduced as

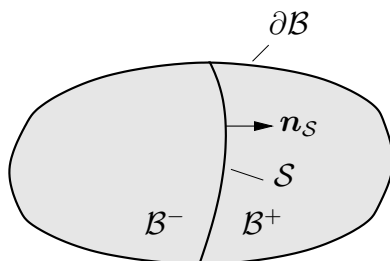


Figure 1: Body with domain wall

$$H(\boldsymbol{\varepsilon}, \mathbf{E}) = \frac{1}{2}(\boldsymbol{\varepsilon} - \boldsymbol{\varepsilon}^0) : [\mathbb{C}(\boldsymbol{\varepsilon} - \boldsymbol{\varepsilon}^0)] - (\boldsymbol{\varepsilon} - \boldsymbol{\varepsilon}^0) : (\mathfrak{b}^T \mathbf{E}) - \frac{1}{2} \mathbf{E} \cdot (\mathbf{A} \mathbf{E}) - \mathbf{P}^0 \cdot \mathbf{E}. \quad (1)$$

It depends on the strain $\boldsymbol{\varepsilon}$ and the electric field \mathbf{E} . The inelastic strain (eigenstrain) $\boldsymbol{\varepsilon}^0$ is introduced to account for point defects and different irreversible strains in the different domains, as will be discussed later. The irreversible polarization is taken into account by the term \mathbf{P}^0 . The elasticity tensor \mathbb{C} , the piezo-electric tensor \mathfrak{b} and the dielectric tensor \mathbf{A} are material constants, which can vary from domain to domain. The electric enthalpy serves as a potential for the symmetric stresses $\boldsymbol{\sigma}$ and the electric displacements \mathbf{D} , i.e.

$$\begin{aligned} \boldsymbol{\sigma} &= \frac{\partial H}{\partial \boldsymbol{\varepsilon}} = \mathbb{C}(\boldsymbol{\varepsilon} - \boldsymbol{\varepsilon}^0) - \mathfrak{b}^T \mathbf{E}, \\ \mathbf{D} &= -\frac{\partial H}{\partial \mathbf{E}} = \mathfrak{b}(\boldsymbol{\varepsilon} - \boldsymbol{\varepsilon}^0) + \mathbf{A} \mathbf{E} + \mathbf{P}^0. \end{aligned} \quad (2)$$

The total potential of the system is now given by internal potential Π^{int} (incorporating H) and the potential Π^{ext} of external forces and external charges.

$$\Pi[\mathbf{u}, \varphi, \mathcal{S}] = \underbrace{\int_{\mathcal{B}^{+/-}} H dV}_{\Pi^{\text{int}}} - \underbrace{\int_{\mathcal{B}} (\mathbf{f} \cdot \mathbf{u} - q\varphi) dV - \int_{\partial \mathcal{B}_t} \mathbf{t}^* \cdot \mathbf{u} dA + \int_{\partial \mathcal{B}_Q} Q^* \varphi dA}_{\Pi^{\text{ext}}} \quad (3)$$

The total potential is a functional of the displacement field \mathbf{u} , the electric potential φ and the position of the domain wall \mathcal{S} . The fields and the position of the domain wall

will be taken into account when computing the variation of the total potential, as the domain wall is assumed to be mobile. The variation of the total potential yields

$$\begin{aligned}
\delta\Pi = & - \int_{\mathcal{B}^{+/-}} (\operatorname{div}\boldsymbol{\sigma} + \mathbf{f}) \cdot \delta\mathbf{u} \, dV - \int_{\mathcal{B}^{+/-}} (\operatorname{div}\mathbf{D} - q)\delta\varphi \, dV \\
& + \int_{\mathcal{B}_t} (\boldsymbol{\sigma}\mathbf{n} - \mathbf{t}^*) \cdot \delta\mathbf{u} \, dA + \int_{\mathcal{B}_Q} (\mathbf{D} \cdot \mathbf{n} + Q^*)\delta\varphi \, dA \\
& - \int_{\mathcal{S}} \underbrace{[(\boldsymbol{\sigma}\mathbf{n}_{\mathcal{S}}) \cdot \delta\mathbf{u}]}_I \, dA - \int_{\mathcal{S}} \underbrace{[(\mathbf{D} \cdot \mathbf{n}_{\mathcal{S}})\delta\varphi]}_II \, dA - \int_{\mathcal{S}} [[H]]\delta w \, dA,
\end{aligned} \tag{4}$$

where the kinematic relation $\boldsymbol{\varepsilon} = \frac{1}{2}(\operatorname{grad}\mathbf{u} + (\operatorname{grad}\mathbf{u})^T)$ and the definition of the electric field $\mathbf{E} = -\operatorname{grad}\varphi$ were used. The variations $\delta\mathbf{u}$ and $\delta\varphi$ vanish on the part of the boundary $\partial\mathcal{B}_u$ or $\partial\mathcal{B}_\varphi$, where either displacement or electric potential boundary conditions are prescribed. In the expressions I and II the following jump relations on the domain wall \mathcal{S} are used

$$[[ab]] = [[a]]\langle\langle b \rangle\rangle + \langle\langle a \rangle\rangle[[b]], \quad [[\delta\mathbf{u}]] = -\delta w[[\operatorname{grad}\mathbf{u}]]\mathbf{n}_{\mathcal{S}}, \quad [[\delta\varphi]] = -\delta w[[\operatorname{grad}\varphi]]\mathbf{n}_{\mathcal{S}} \tag{5}$$

to obtain

$$\begin{aligned}
[[\boldsymbol{\sigma}\mathbf{n}_{\mathcal{S}}] \cdot \delta\mathbf{u}] &= [[\boldsymbol{\sigma}]]\mathbf{n}_{\mathcal{S}} \cdot \langle\langle\delta\mathbf{u}\rangle\rangle - \langle\langle\boldsymbol{\sigma}\mathbf{n}_{\mathcal{S}}\rangle\rangle[[\operatorname{grad}\mathbf{u}]]\mathbf{n}_{\mathcal{S}}\delta w \\
[[\mathbf{D} \cdot \mathbf{n}_{\mathcal{S}}]\delta\varphi] &= [[\mathbf{D}]] \cdot \mathbf{n}_{\mathcal{S}}\langle\langle\delta\varphi\rangle\rangle - \langle\langle\mathbf{D} \cdot \mathbf{n}_{\mathcal{S}}\rangle\rangle[[\operatorname{grad}\varphi]]\mathbf{n}_{\mathcal{S}}\delta w.
\end{aligned} \tag{6}$$

Note that δw is the variation of the domain wall in normal direction. Thus the variation of the total potential becomes

$$\begin{aligned}
\delta\Pi = & - \int_{\mathcal{B}^{+/-}} (\operatorname{div}\boldsymbol{\sigma} + \mathbf{f}) \cdot \delta\mathbf{u} \, dV - \int_{\mathcal{B}^{+/-}} (\operatorname{div}\mathbf{D} - q)\delta\varphi \, dV \\
& + \int_{\partial\mathcal{B}_t} (\boldsymbol{\sigma}\mathbf{n} - \mathbf{t}^*) \cdot \delta\mathbf{u} \, dA + \int_{\partial\mathcal{B}_Q} (\mathbf{D}\mathbf{n} - Q^*)\delta\varphi \, dA \\
& - \int_{\mathcal{S}} ([[\boldsymbol{\sigma}]]\mathbf{n}_{\mathcal{S}}) \cdot \langle\langle\delta\mathbf{u}\rangle\rangle \, dA - \int_{\mathcal{S}} ([[\mathbf{D}]]\cdot \mathbf{n}_{\mathcal{S}})\langle\langle\delta\varphi\rangle\rangle \, dA \\
& - \int_{\mathcal{S}} ([[H]] - \langle\langle\boldsymbol{\sigma}\mathbf{n}_{\mathcal{S}}\rangle\rangle[[\operatorname{grad}\mathbf{u}]]\mathbf{n} - \langle\langle\mathbf{D} \cdot \mathbf{n}_{\mathcal{S}}\rangle\rangle[[\operatorname{grad}\varphi]]\mathbf{n}_{\mathcal{S}})\delta w \, dA.
\end{aligned} \tag{7}$$

Arbitrary variations $\delta\mathbf{u}$, $\delta\varphi$, $\langle\langle\delta\mathbf{u}\rangle\rangle$, $\langle\langle\delta\varphi\rangle\rangle$ yield the equilibrium equations

$$\begin{aligned}
\operatorname{div}\boldsymbol{\sigma} + \mathbf{f} &= \mathbf{0} & \text{in } \mathcal{B}^{+/-}, \\
[[\boldsymbol{\sigma}]]\mathbf{n}_{\mathcal{S}} &= \mathbf{0} & \text{on } \mathcal{S}
\end{aligned} \tag{8}$$

and the electro-static relations

$$\begin{aligned}
\operatorname{div}\mathbf{D} - q &= 0 & \text{in } \mathcal{B}^{+/-}, \\
[[\mathbf{D}]] \cdot \mathbf{n}_{\mathcal{S}} &= 0 & \text{on } \mathcal{S}
\end{aligned} \tag{9}$$

in the bulk and on the domain wall together with the respective Neumann boundary conditions:

$$\boldsymbol{\sigma}\mathbf{n} = \mathbf{t}^* \quad \text{on } \partial\mathcal{B}_t \quad \text{and} \quad \mathbf{D}\mathbf{n} = -Q^* \quad \text{on } \partial\mathcal{B}_Q. \quad (10)$$

Thus in equilibrium and under electrostatic conditions the variation can be written compactly as

$$\delta\Pi = - \int_{\mathcal{S}} \underbrace{(\mathbf{n}_{\mathcal{S}} \cdot ([\boldsymbol{\Sigma}]\mathbf{n}_{\mathcal{S}}))}_{\tau_n} \delta w \, dA, \quad (11)$$

where the energy-momentum tensor (or the Eshelby-stress tensor) is introduced

$$\boldsymbol{\Sigma} = H\mathbf{1} - (\text{grad}\mathbf{u})^T \boldsymbol{\sigma} - \text{grad}\varphi \otimes \mathbf{D} \quad (12)$$

and a (scalar) driving force τ_n is identified as

$$\tau_n = \mathbf{n}_{\mathcal{S}} \cdot ([\boldsymbol{\Sigma}]\mathbf{n}_{\mathcal{S}}). \quad (13)$$

This motivates that the domain wall will always move according to the driving force τ_n , to reduce the total potential. It is emphasized here, that from energy considerations and the variational procedure presented here the kinetic relation between the domain wall movement and the driving force cannot be deduced.

3 POINT DEFECTS

Point defects model on the continuum level the occurrence of a foreign atom or a vacancy. Such defects disturb the deformation and charge state of the otherwise homogeneous material. To model a point defect in the mechanical sense it is associated with an inelastic eigenstrain that is localized at the position \mathbf{x}^D of the point defect (center of dilatation)

$$\boldsymbol{\varepsilon}^0 \rightarrow \alpha \mathbf{1} \delta(\mathbf{x} - \mathbf{x}^D). \quad (14)$$

The parameter α represents the strongness of the mechanical defect. For $\alpha \geq 0$ a foreign atom is modeled that is too large/small for the surrounding crystal lattice. The inelastic strain is assumed to be isotropic. It will enter the problem through the constitutive equations (2).

In the electric setting the point defect is modeled a a localized volume charge

$$q \rightarrow \beta \delta(\mathbf{x} - \mathbf{x}^D), \quad (15)$$

with the density β . In the electric sense the point defect will be considered on the level of the balance equations (9)₁.

4 EXAMPLES

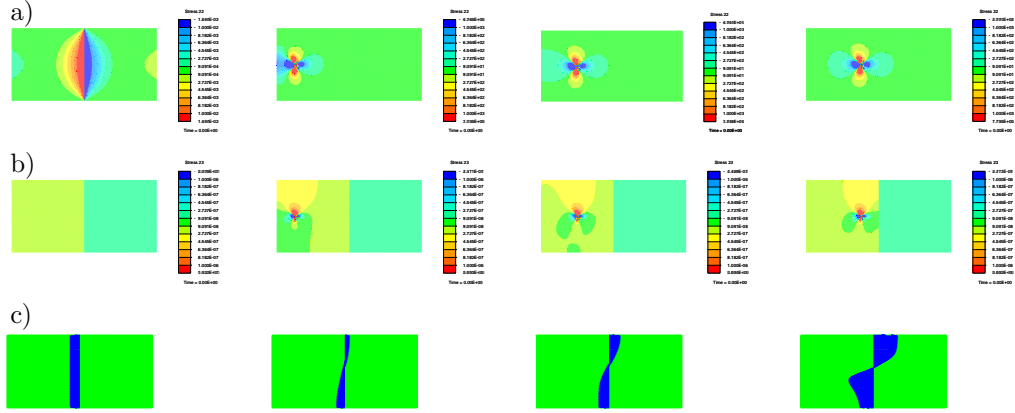


Figure 2: Interaction of domain wall and point defect: a) stress σ_{22} , b) electric displacement D_2 , c) driving force τ_n

The material data are chosen to mimic the piezo-electric behavior of PZT. The point defect properties are set to model a positively charged vacancy, i.e. $\alpha < 0$ and $\beta > 0$. The sample problem consists of a rectangular region of $100 \text{ nm} \times 200 \text{ nm}$ size with a 180° domain wall. The left domain is polarized upwards, while in the right domain the irreversible polarization \mathbf{P}^0 points downwards. The system is loaded by a potential difference of 600 V/mm in the vertical direction. The vertical boundaries are insulated, i.e. $\mathbf{D} \cdot \mathbf{n} = 0$. With respect to the mechanical fields traction free conditions are assumed everywhere.

Fig. 2 shows the results for no point defect and a point defect which is located at a distance of 75, 50 and 25 nm from the domain wall. The point defect causes much higher stress levels than the inhomogeneity in the defect free state, therefore the levels of the contours for the σ_{22} plots were changed. Also in the plots of the driving force the scaling of the arrows was changed to ensure a good visibility of the driving force distribution.

The intensity of the interaction of the domain wall and the defect increases when the defect approaches the domain wall. But even in the situation, where the defect is positioned far away from the domain wall, the sign of the driving force τ_n is changed in the upper half of the domain wall. Thus the overall driving force defined as

$$T_n = \int_S \tau_n dA \quad (16)$$

decreases as compared to the situation where no defect is present. In fig. 3 the re-

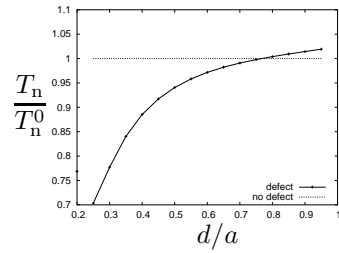


Figure 3: Resulting driving force on a domain wall

sulting driving force T_n is analysed as a function of the distance d between the defect and the domain wall. The resulting driving force T_n is normalized with the resulting driving force of the defect free situation T_n^0 . The reference length a is the height of the domain wall. From fig. 3 it can be seen, that the driving force is reduced by about 30% if the defect approaches the domain wall. If domain wall and defect become closer the numerical resolution of the fields and the strong gradients in the vicinity of the defect become poor, therefore no trustworthy results are obtained in this strong interaction case. But the trend is obvious, the occurrence of point defects reduces the driving force and therefore has the possible capability to block domain walls and pin them. In order to move the domain wall a higher external field, i.e. potential difference, is needed.

It is also mentioned that by increasing the point defect concentration the domain wall can finally be stopped. If point defects are placed randomly in the left domain the resulting driving force will be reduced. For this set of parameter about seven point defects will be strong enough to change the sign in the total driving force, thereby stopping the domain wall.

REFERENCES

- [1] G. A. Maugin. *Material Inhomogeneities in Elasticity*. Chapman & Hall, London, Glasgow, New York, Tokyo, Melbourne, Madras, 1993.
- [2] M. E. Gurtin. *Configurational forces as basic concept of continuum physics*. Springer, Berlin, New York, Heidelberg, 2000.
- [3] R. Kienzler and G. Herrmann. *Mechanics in Material Space*. Springer, New York, Berlin, Heidelberg, 2000.
- [4] R. Mueller, S. Kolling, and D. Gross. On configurational forces in the context of the Finite Element Method. *Int. J. Numer. Meth. Engng.*, 53:1557–1574, 2002.
- [5] R. Mueller and G.A. Maugin. On material forces and finite element discretizations. *Comp. Mechanics*, 29(1):52–60, 2002.
- [6] J. Nuffer, D.C. Lupascu, and J. Rödel. Damage evolution in ferroelectric PZT induced by bipolar electric cycling. *Acta mater.*, 48:3783–3794, 2000.
- [7] R. Mueller, S. Eckert, and D. Gross. 3D equilibrium shapes of periodically arranged anisotropic precipitates with elastic misfit. *Archive of Mechanics*, 52(4–5):663–683, 2000.